6

Functional Assessment of Individual Lung Lobes with MDCT Images

Syoji Kobashi, Kei Kuramoto and Yutaka Hata
University of Hyogo
Japan

1. Introduction

CT is an effective modality for evaluating the structure inside the body and the 3-D shape of organs of interest because of ability of high spatial resolution and of high acquisition speed. However, CT is weak to evaluate a function of organs because CT only maps X-ray absorption coefficients of materials constructing human body. Therefore, study of functional imaging of organs by using CT images will be a breakthrough of image diagnosis. This chapter introduces a novel method for estimating pulmonary function using MDCT.

The human lung is composed of five anatomical compartments called "lung lobes." The right lung is segmented into three lung lobes (the upper, middle and lower lobes), and the left lung is segmented into two lung lobes (the upper and lower lobes). Thoracic surgeries such as a living-donor lobar lung transplantation (LDLLT) (Date et al., 2003a) and the lobectomy (Kirby et al., 1993) often operate by a lung lobe. LDLLT is an operation that transplants the right and left lower lobes of two living donors to a recipient. In this surgery, predicting the postoperative forced vital capacity (FVC) of a recipient is necessary to select the adequate donors. The lobectomy is a treatment that extirpates lung lobe. This surgery excises the diseased region such as lung or improves breathing function by reducing the lung capacity that overexpands by emphysema. In this surgery, predicting the postoperative FVC is necessary to investigate the effectiveness of the surgery, too. Since these surgeries treatment lobe by lobe, the prediction should be based on individual lung lobes. Although a spirometry, which is widely used in a clinical field, enables us to measure the FVC of whole lung, it is not available for the FVCs of the individual lung lobes.

Date et al. have proposed a method for approximating FVCs of individual lung lobes by determining the contribution ratio to FVC of the whole lung (Date et al., 2003b). The contribution ratio is determined from the number of lung segments occupied in the lung lobe. The FVC of recipients that underwent the LDLLT measured at 6 months was correlated well with the grafts FVCs of donors estimated by their method ($r = 0.802$). However, the method does not consider the variation of the lobar function among subjects. To consider such variation, a tracheal tube can measure the FVCs of the right and the left lung respectively. However, the method is invasive due to the use of anesthesia and the tracheal tube, and it still cannot measure the FVCs of the individual lung lobes.

This chapter proposes a novel method for measuring the FVCs of individual lung lobes by using volume data acquired from CT scanner. This approach is based on an assumption that the FVC of whole lung can be expressed as the change of lung lobe volumes between

inspiratory and expiratory. Thus, the contribution ratio of lung lobes can be obtained by measuring the volumes of lung lobes for each of inspiratory lung and of expiratory lung. Because of the use of MDCT images, the proposed method is less invasive in comparison with the use of the tracheal tube. The proposed method can consider the variation of the lobar function among subjects.

There are several segmentation methods of lung lobes from MDCT images. Zhou et al. (Zhou et al., 2004) and Saita et al. (Saita et al., 2004) extract the lobar fissures in MDCT images to determine the boundary surface between lung lobes. They are called LFB (lobar fissure based) method. Because lobar fissure indicates right boundary surface of lung lobe, this approach is high accuracy. However, this approach has two limitations; (1) it is limited to apply the method by a lack of the lobar fissures, and (2) false positive (FP) regions of lobar fissures will be extracted.

To overcome the difficulty of lacked lobar fissures, we proposed a new method (Kobashi et al., 2010) that estimates the boundary surface between the lung lobes with the tubular tissue density, which is called TTB (tubular tissue density based). The tubular tissues consist of the peripheral blood vessels and peripheral bronchus. Because the tubular tissues do not cross over the boundary surface between the lung lobes, this method defines the boundary surface as the region where the tubular tissue density is low. Therefore, this approach can be applied to MDCT images that have a lack of lobar fissures.

2. Method

2.1 Image acquisition and forced vital capacity measurement of the whole lung

MDCT images were acquired from an MDCT scanner (LightSpeed Ultra16, GE Medical Systems, WI, USA). The acquisition parameters for the chest MDCT images were: the tube voltage was 120 kV; the tube current was 440 mA; the field of view (FOV) was 360 mm; the matrix size was 512 × 512 pixels; the slice thickness was 0.625 mm and was with no gap. Each sliced image included volumetric data, and a volume dataset from the apex of the lung to the diaphragmatic surface was composed of over 450 contiguous axial planes. Given these conditions, the acquisition time requiring breath holding was about 10 sec. Fig. 1 shows raw MDCT images of the chest.

Two sets of MDCT image were acquired with inspiratory condition and with expiratory condition. For each dataset, the proposed method segmentes the lung lobes, and measrues

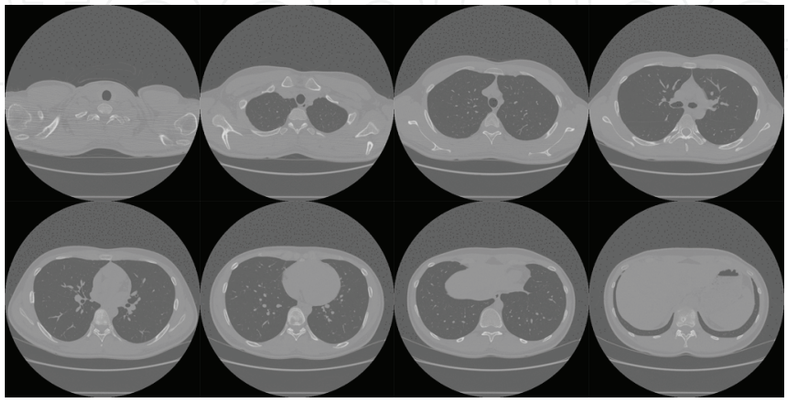

Fig. 1. Raw MDCT images of the chest. Upper-left to lower-right are superior to inferior.

the individual volumes. Thus, we can estimate the change of lung lobe volumes between the inspiratory and the expiratory conditions. The contribution rate for the whole lung capacity can be estaimated. By using the whole lung FVC measured by a spirometer, the individual lung FVCs are estimated.

2.2 Image analysis

This study defines tubular tissues as a set of peripheral blood vessels and peripheral bronchi. Because the tubular tissues do not exist on the boundary between the lung lobes, the method determines the boundary by finding a 3-D continuous space where few tubular tissues exist. Therefore, the method does not depend on detection accuracy of the lobar fissures from MDCT images. The finding process is automatically performed with a fuzzy control (Kobashi et al., 2010), and is composed from the following steps. They are applied to both of MDCT datasets with inspiratory and with expiratory conditions.

Step 1. Segment the lung region from MDCT images.

The lung region is segmented by 3-D region growing (RG) and morphological operation which consists of 3-D erosion and dilation methods. The bronchial region is removed from the segmented region by extracting the air region inside the bronchial walls using 3-D RG according to the method proposed by Mori et al. (2000).

Step 2. Extract the tubular tissues.

The peripheral blood vessels have higher CT values than the surrounding parenchyma, and the peripheral bronchi also have high CT values. In summary, tubular tissues have high CT values in the lung region. Thus, the peripheral blood vessels and peripheral bronchi are collectively extracted and are called tubular tissues. They are extracted by an adaptive thresholding using mean of a local window. Fig. 2 shows an example of the extracted tubular tissues. Then, tubular tissue density is calculated for each voxel in the lung region.

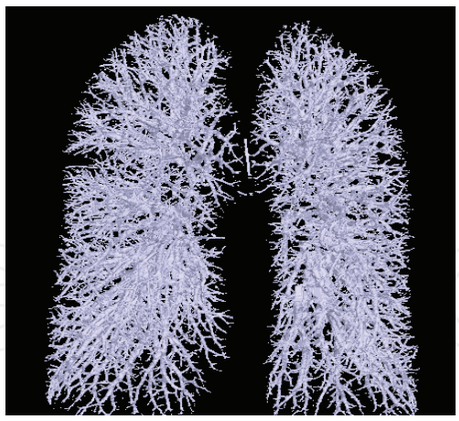

Fig. 2. 3-D rendering image of the extracted tubular tissues.

Step 3. Determine the initial surface.

An examiner gives a plane, which runs a space where few tubular tissues using a configured graphical user interface (GUI). The GUI displays the 3-D rendering images of the extracted tubular tissues. The examiner rotates the rendering image to find a space with few tubular tissues. As shown in Fig. 3, by giving a straight line on the rendering image, a plane forwarding to the view angle is obtained as the initial surface of the boundary between the lung lobes.

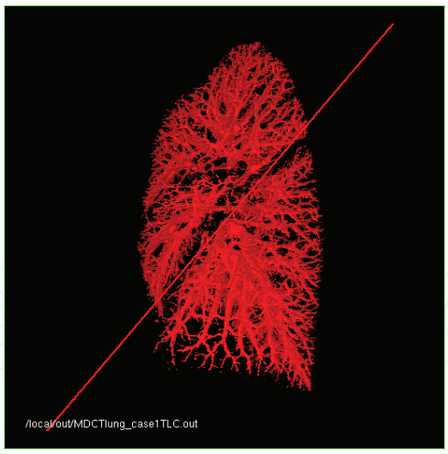

Fig. 3. Manual determination of initial surface using the configured GUI. This figure shows the rendering image of tubular tissues in the right lung. Two cracks of tubular tissues corresponding to the major and minor fissures can be found. The examiner rotates the rendering image and gives a straight line on the rendering image.

Step 4. Deform the curved surfaces and obtain the boundaries.
The initial surface is converted into trapezoidal mesh. By moving the vertexes of the mesh, the surface can be deformed. The movement of the vertexes is automatically performed with fuzzy control system, which evaluates the anatomical knowledge on the lobar boundaries: (1) the moving vertex moves toward a space with low tissue density, and (2) the deforming surface model maintains a smoothed surface. The anatomical knowledge is described by fuzzy IF-THEN rules (e.g., Han et al., 2007), and the vertexes are moved to a position with the higher fuzzy degree belonging to the lobar boundaries.
Step 5. Segment the lung lobes by the obtained boundaries.
Step 3 and step 4 are applied to determine one boundary for the left lung, and to determine two boundaries for the right lung. Using the boundaries, the left lung is decomposed into the upper and the lower lung lobes, and the right lung is decomposed into the upper, the middle, and the lower lung lobes.

2.3 Estimation of individual forced vital capacity

This approach is based on an assumption that the FVC of whole lung is collerated with the differences of volumes between inspiratory and expiratory. The proposed method can calculate volumes of the individual lung lobes from a set of MDCT images on inspiratory and expiratory of the same subject. Therefore, by using the volumes of the segmented lung lobe region, it is possible to estimate the FVCs of individual lung lobes.
We consider that the FVC of whole lung is the sum of the FVCs of individual lung lobes. If we can calculate the ratios that each lung lobe can contribute to the FVC of whole lung, the FVCs of individual lung lobes are predicted. The contribution ratios are associated with the volume differences of the segmented lung lobe region between inspiratory and expiratory. Therefore, the FVCs of individual lung lobes are estimated by using the FVC of whole lung measured by the spirometry and the contribution ratios.
The proposed method defines the contribution ratio of the lung lobe of interest R(t) (t = {the right upper lobe, right middle lobe, right lower lobe, left upper lobe, and left lower lobe}) through the following equation,

$$R(t) = \frac{V_i(t) - V_e(t)}{\sum_{q \in t} V_i(q) - V_e(q)} \quad (1)$$

where *Vi* and *Ve* are the inspiratory and expiratory volume of the segmented lung lobe region, respectively. In consequently, the FVCs of individual lung lobes FVC(t) are predicted in the following equation,

$$FVC(t) = R(t) \cdot FVC_{lung} \quad (2)$$

where FVC_{lung} denotes the FVC of whole lung measured by the spirometry, and sum of contirbution ratios equals to 1. Therefore, the sum of *FVC(t)* equals FVC_{lung}. Because of the use of the image information (*i.e.*, chest MDCT images), *R(t)* can reflect the variation of the respiratory function among subjects in comparison with the conventional method that fixes the contribution ratio (Date et al., 2003b).

4. Experimental results

The proposed method was applied to four normal subjects who were recruited in our institute. Table I shows the profiles of the subjects. All the subjects provided written informed consent according to a guideline approved by the local Ethics Committee. In the eight collected MDCT datasets, there were partial lacks in the delineation of the lobar fissure.

Subjects	Sex	Age (YO)	Height (cm)	Smoking History	VCP (cc)	FVC (cc)	FEV1% (%)
A	Male	23	175	No	4380	3440	87
B	Male	23	172	No	4300	3780	91
C	Male	22	173	No	4350	2890	99
D	Male	21	178	Yes	4490	3980	91

Table I. Subject profiles; YO means years old, VCP means vital capacity predicted, and FEV1% means ratio of FEV1 (forced expiratory volume in one second) to FVC.

Fig. 3 shows raw MDCT images, the experimental results with the proposed method, and lobar fissures extracted by conventional method for comparison. In raw MDCT image, lobar fissures appear with the higher CT values than the surrounding region. However, over-extraction and under-extraction tend to be occurred. In contrast, the proposed method determines the lobar boundaries for the lacked fissures.

To evaluate the determined boundaries with the proposed method, they were compared with boundaries manually delineated by a physician. Because the proposed method requires an interaction to determine the initial surface, for each dataset, the proposed method was applied 10 times. Table II shows the comparison results for each boundary; the left major fissure, the right major fissure, and the right minor fissure. The accuracy was evaluated by measuring the shortest distance between the automatically determined boundary and the manually delineated boundary. The mean ± standard deviation (SD) of detecting accuracy was 3.20 ± 1.72 [mm].

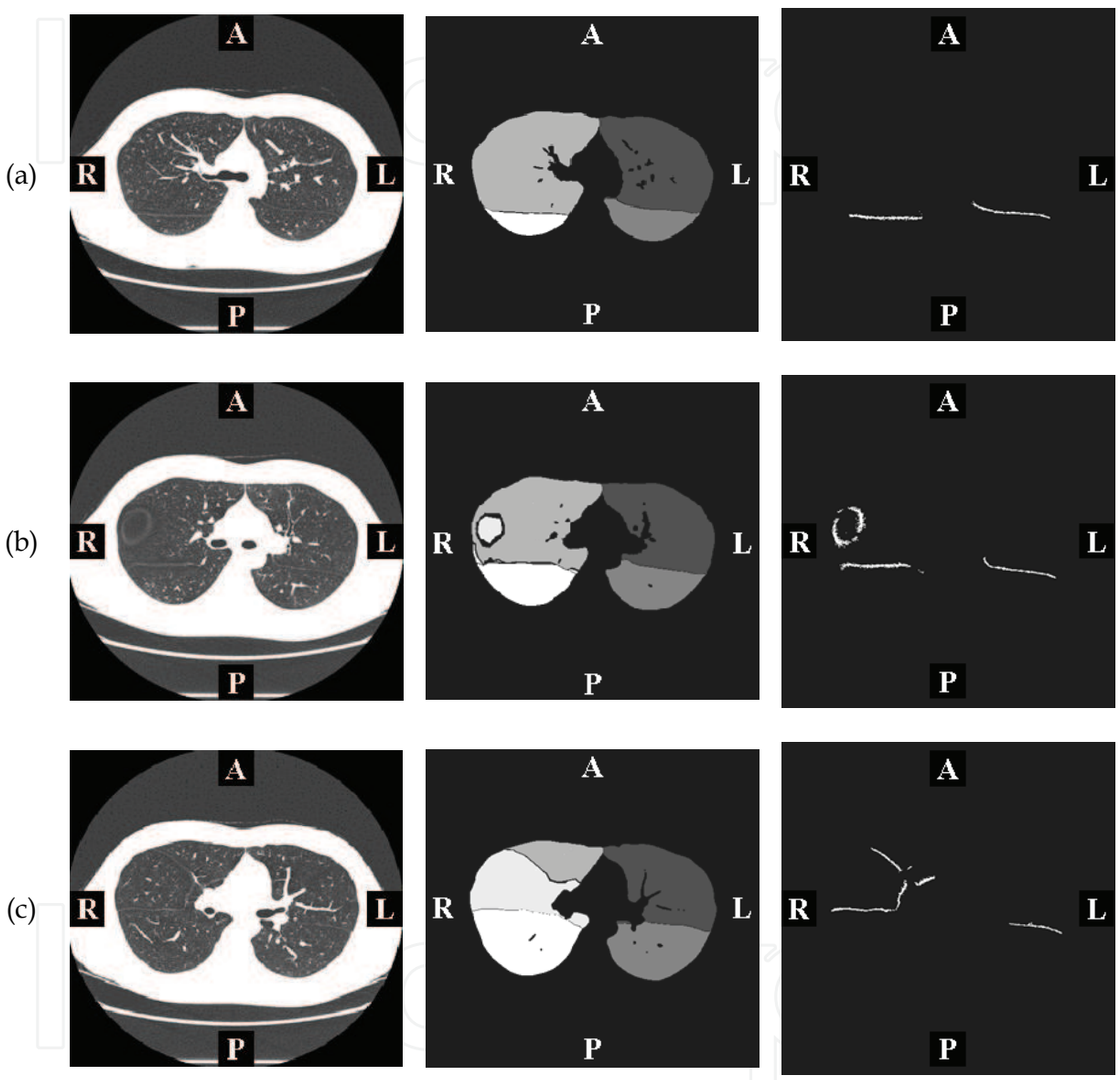

Fig. 3. 2-D segmentation results of subject A. (a) 170th slice, (b) 186th slice, and (c) 212th slice; (left) raw MDCT images, (middle) lung lobes segmented with the proposed method, (right) extracted lobar fissures with the conventional method.

		Left Major	Right Major	Right Minor
Subject A	Inspiratory	3.29±1.83	3.62±1.69	2.87±1.78
	Expiratory	3.34±1.75	3.43±1.68	2.60±1.62
Subject B	Inspiratory	3.29±1.68	3.54±1.69	3.62±1.72
	Expiratory	3.16±1.76	3.39±1.67	3.33±1.68
Subject C	Inspiratory	2.71±1.79	3.37±1.75	3.19±1.80
	Expiratory	3.09±1.63	3.33±1.68	2.69±1.71
Subject D	Inspiratory	3.65±1.65	3.06±1.79	3.49±1.76
	Expiratory	3.05±1.71	2.94±1.75	2.83±1.82

Table II. Accuracy of detecting lobar boundaries with the proposed method (mean ± standard deviation [mm]).

Fig. 4 shows the surface shaded display (SSD) images of the segmented lung lobes. For any subject, and for any condition of inspiratory or expiratory, the lung lobes were segmented well. The comparison of lung lobes between the conditions of inspiratory and expiratory demonstrates that the lobes deform largely by inspiration. Next, by counting the number of voxels for each lung lobe, the volumes can be measured. Table III shows the lung lobe volumes estimated by the proposed method. To validate the proposed method, lung lobe volumes were measured manually by delineating the lung lobe boundaries with physicians. Error ratio is computed by $\frac{truth - estimated}{truth}$. The absolute mean error ratio across the lung lobes on the inspiratoy condition was 0.9 % and on the expiratory condition was 1.2 %, and the mean was 1.1 %. As shown in this table, there are no differences of segmentation accuracy among subjects, lung lobes, and inspiratory/expiratory conditions.

Using the estimated lung lobe volumes shown in Table III, contribution ratio was calculated by Eq. (1). The contribution ratios calculated with the present method, and the fixed contribution ratios introduced by Data et al. (2003b) are shown in Table IV. There are slight differences between the estimated contribution ratios and the fixed parameters: e.g., the contribution ratio of the right middle lobe was lower than the fixed one, and the right lower lobe was higher than the fixed one. In addition, we can show the differences of contribution ratios among the subjects.

Finally, FVCs of lung lobes were estimated by using Eq. (2). Table V shows the estimated FVCs of the individual lung lobes for all subjects. By using this table, we may predict FVC after LDLLT. For example, assume the left lower lobe of subject A and the right lower lobe of subject B are transplanted into a recipient. In this case, after LDLLT, FVC of the recipient can be predicted as 2217.4 cc (=1026.2 cc + 1191.1 cc), and FVC of two donors, subject A and subject B, will be 2413.8 cc (=3440 cc – 1026.2 cc) and 2588.9 cc (=3780cc -1191.1 cc), respectively. In the similar way, FVC after LDLLT with the other combination of donors can be predicted. Thus, by using this technique, we might choose the better donors for the recipient. Of course, FVC after LDLLT will be affected by the other factors. Therefore, we should validate this technique in the future.

(a) Subject A.

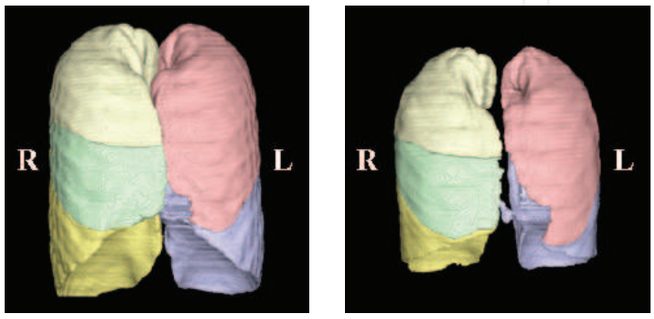

(b) Subject B.

(c) Subject C.

(d) Subject D.

Fig. 4. SSD images of segmentation results; left and right; the segmentation results of a subject with inspiratory and expiratory, respectively. Different lung lobes are displayed with the different colours.

			Left Upper	Left Lower	Right Upper	Right Middle	Right Lower
A	Inspiratory	Truth	1157	1408	938	451	1604
		Estimated	1169	1396	937	452	1604
		error ratio	1.0%	-0.9%	-0.1%	0.2%	0.0%
	Expiratory	Truth	683	645	565	298	883
		Estimated	673	655	571	294	881
		error ratio	-1.5%	1.6%	1.1%	-1.3%	-0.2%
B	Inspiratory	Truth	1207	1709	937	496	1814
		Estimated	1213	1703	942	493	1811
		error ratio	0.5%	-0.4%	0.5%	-0.6%	-0.2%
	Expiratory	Truth	740	834	561	338	945
		Estimated	744	830	571	326	946
		error ratio	0.5%	-0.5%	1.8%	-3.6%	0.1%
C	Inspiratory	Truth	1058	1111	779	362	1266
		Estimated	1039	1130	771	348	1288
		error ratio	-1.8%	1.7%	-1.0%	-3.9%	1.7%
	Expiratory	Truth	584	479	440	205	636
		Estimated	575	487	426	210	644
		error ratio	-1.5%	1.7%	-3.2%	2.4%	1.3%
D	Inspiratory	Truth	1150	1486	999	454	1661
		Estimated	1168	1469	993	458	1665
		error ratio	1.6%	-1.1%	-0.6%	0.9%	0.2%
	Expiratory	Truth	623	684	530	277	817
		Estimated	623	684	535	275	812
		error ratio	0.0%	0.0%	0.9%	-0.7%	-0.6%
Inspiratory		absolute mean	1.2%	1.0%	0.6%	1.4%	0.5%
Expiratory		absolute mean	0.9%	0.9%	1.7%	2.0%	0.6%
Total		absolute mean	1.1%	1.0%	1.2%	1.7%	0.5%

Table III. Estimated lung lobe volumes with the proposed method (cc).

Subject	Left Upper	Left Lower	Right Upper	Right Middle	Right Lower
A	20.0%	29.8%	14.7%	6.4%	29.1%
B	17.1%	31.8%	13.5%	6.1%	31.5%
C	20.8%	28.8%	15.4%	6.2%	28.8%
D	19.3%	27.8%	16.2%	6.5%	30.2%
Mean	19.3%	29.6%	15.0%	6.3%	29.9%
Conv. fixed parameter	21.1% (=4/19)	26.3% (=5/19)	15.8% (=3/19)	10.5% (=2/19)	26.3% (=5/19)

Table IV. Estimated contribution ratios of the individual lung lobes. "Conv. fixed parameters" are parameters introduced by Data et al (2003b).

Subject	Whole lung	Left Upper	Left Lower	Right Upper	Right Middle	Right Lower
A	3440	686.9	1026.2	506.9	218.8	1001.3
B	3780	645.8	1202.2	510.9	230.0	1191.1
C	2890	600.3	831.8	446.3	178.5	833.1
D	3980	768.1	1106.3	645.5	257.9	1202.2

Table V. Estimated FVCs of lung lobes with the proposed method (cc). The whole lung FVC was measured by spirometry, and the others were estimated by the proposed method.

7. Conclusion

This chapter presents a novel method for estimating individual lung lobe FVC with MDCT images. The new method can be applied to chest MDCT images with lacked fissures. Moreover, this will be the first attempt to estimate the individual lung lobe FVC. In the future, we should validate the estimated individual lung lobe FVC. In addition, the effectiveness of this technique will be discussed through future clinical studies.

8. References

Date, H.; Aoe, M.; Nagahiro, I.; Sano, Y.; Andou, A.; Matsubara, H.; Goto, K.; Tedoriya, T. & Shimizu, N. (2003). Living-donor lobar lung transplantation for various lung diseases, *The Journal of Thoracic and Cardiovascular Surgery*, Vol. 126, No. 2, pp. 476-481.

Date, H.; Aoe, M.; Sano, Y.; Nagahiro, I.; Andou, A.; Matsubara, H.; Goto, K.; Tedoriya, T. & Shimizu, N. (2003). How to predict forced vital capacity of the recipient after living-donor lobar lung transplantation, *The Journal of Heart and Lung Transplantation*, Vol. 22, No. 1, pp. S181-S181.

Han, H. & Ikuta, A. (2007) Returning to the Starting Point of the "Fuzzy Control", *Int. J. Innovative Computing, Information and Control*, vol.3, no.2, pp.319-333.

Kirby, T. J. & Rice, T. W. (1993). Thoracoscopic lobectomy, *The Annals of Thoracic Surgery*, Vol. 56, pp.784-786.

Kobashi, S. & Hata, Y. (2010). Lung Lobar Segmentation Using Tubular Tissue Density from Multidetector-row CT images, *International Journal of Innovative Computing, Information and Control*, Vol. 6, No. 3(A), pp. 829-842.

Mori, K.; Hasegawa, J.; Suenaga Y. & Toriwaki, J. (2000). Automated anatomical labeling of the bronchial branch and its application to the virtual bronchoscopy system, *IEEE Trans. on Medical Imaging*, Vol.19, No.2, pp.103-114.

Saita, S.; Yasutomo, M.; Kubo, M.; Kawata, Y.; Niki, N.; Eguchi, K.; Ohmatsu, H.; Kakinuma, R.; Kaneko, M.; Kusumoto, M.; Moriyama, N. & Sasagawa, M. (2004). An extraction algorithm of pulmonary fissures from multi-slice CT image, *Proc. SPIE Conf. Medical Imaging*, Vol. 5370, pp. 1590–1597.

Zhou, X.; Hayashi, T.; Hara, T.; Fujita, H.; Yokoyama, R.; Kiryu, T. & Hoshi, H. (2004). Automatic recognition of lung lobes and fissures from multi-slice CT images, *Proc. SPIE Conf. Medical Imaging*, Vol. 5370, pp. 1629–1633.

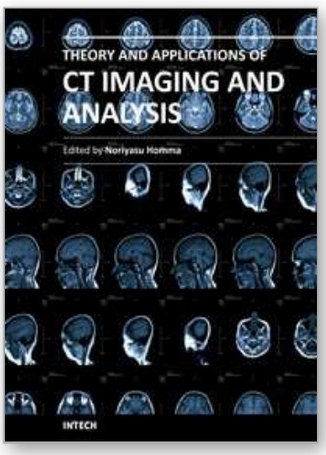

Theory and Applications of CT Imaging and Analysis
Edited by Prof. Noriyasu Homma

ISBN 978-953-307-234-0
Hard cover, 290 pages
Publisher InTech
Published online 04, April, 2011
Published in print edition April, 2011

The x-ray computed tomography (CT) is well known as a useful imaging method and thus CT images have continuingly been used for many applications, especially in medical fields. This book discloses recent advances and new ideas in theories and applications for CT imaging and its analysis. The 16 chapters selected in this book cover not only the major topics of CT imaging and analysis in medical fields, but also some advanced applications for forensic and industrial purposes. These chapters propose state-of-the-art approaches and cutting-edge research results.

How to reference
In order to correctly reference this scholarly work, feel free to copy and paste the following:

Syoji Kobashi, Kei Kuramoto and Yutaka Hata (2011). Functional Assessment of Individual Lung Lobes with MDCT Images, Theory and Applications of CT Imaging and Analysis, Prof. Noriyasu Homma (Ed.), ISBN: 978-953-307-234-0, InTech, Available from: http://www.intechopen.com/books/theory-and-applications-of-ct-imaging-and-analysis/functional-assessment-of-individual-lung-lobes-with-mdct-images

INTECH
open science | open minds

InTech Europe
University Campus STeP Ri
Slavka Krautzeka 83/A
51000 Rijeka, Croatia
Phone: +385 (51) 770 447
Fax: +385 (51) 686 166
www.intechopen.com

InTech China
Unit 405, Office Block, Hotel Equatorial Shanghai
No.65, Yan An Road (West), Shanghai, 200040, China
中国上海市延安西路65号上海国际贵都大饭店办公楼405单元
Phone: +86-21-62489820
Fax: +86-21-62489821

IntechOpen